

Arc-length and explicit methods for static analysis of prestressed concrete members

Bulent Mercan^{*1}, Henryk K. Stolarski^{2a} and Arturo E. Schultz^{2b}

¹*2H Offshore Inc., 15990 N Barkers Landing #200, Houston, TX 77079, USA*

²*Department of Civil, Environmental, and Geo-Engineering, Univ. of Minnesota,
500 Pillsbury Drive SE Minneapolis, MN 55455, USA*

(Received July 21, 2015, Revised February 29, 2016, Accepted March 24, 2016)

Abstract. This paper compares the arc-length and explicit dynamic solution methods for nonlinear finite element analysis of prestressed concrete members subjected to monotonically increasing loads. The investigations have been conducted using an L-shaped, prestressed concrete spandrel beam, selected as a highly nonlinear problem from the literature to give insight into the advantages and disadvantages of these two solution methods. Convergence problems, computational effort, and quality of the results were investigated using the commercial finite element package ABAQUS. The work in this paper demonstrates that a static analysis procedure, based on the arc-length method, provides more accurate results if it is able to converge on the solution. However, it experiences convergence problems depending upon the choice of mesh configuration and the selection of concrete post-cracking response parameters. The explicit dynamic solution procedure appears to be more robust than the arc-length method in the sense that it provides acceptable solutions in cases when the arc-length approach fails, however solution accuracy may be slightly lower and computational effort may be significantly larger. Furthermore, prestressing forces must be introduced into the finite element model in different ways for the explicit dynamic and arc-length solution procedures.

Keywords: finite element analysis; prestressed; concrete; cracking; tension stiffening; arc-length method; riks method; explicit dynamic method

1. Introduction

Even though experimental methods still play a key role in research, numerical methods are increasingly replacing experiments due to their lower cost and time requirements when compared to experiments. Highly nonlinear problems can be solved by using commercially available computer finite element software. Nevertheless, finite element analysis, particularly nonlinear analysis, requires the knowledge of how various modeling techniques might affect the numerical results. For example, a three-dimensional finite element simulation of a prestressed concrete beam

*Corresponding author, Ph. D., E-mail: bulent.mercan@2hoffshoreinc.com

^aProfessor; E-mail: stola001@umn.edu

^bProfessor, E-mail: schul088@umn.edu

inherently introduces modeling challenges since the analysis model needs to provide a solution for the complex material response of concrete using an appropriate numerical solution method.

Concrete is a strongly nonlinear material and causes many numerical difficulties in finite element analysis (Prinjha and Shepherd 2003, Thevendran *et al.* 1999). The stress-strain relation of concrete under uniaxial tension features a peak value for the tensile strength followed by a sudden drop with negative stiffness. In uniaxial compression, the stress-strain relation contains a strain hardening branch up to the compressive strength of the concrete and a strain softening regime thereafter. Cracking in tension and crushing in compression are irreversible processes that can be defined as damage. These characteristics of concrete constitute the sources of nonlinearity and numerical challenges for finite element analysis.

Academic research dedicated to the analysis of concrete materials and structures is vast and still undergoing further development. Various approaches for modeling of concrete are investigated in such research ranging from continuum plasticity and damage (Jirásek and Grassl 2008, Grassl and Jirásek 2006) to those capturing initiation and propagation of discrete cracks (Grassl and Rempling 2007). Various numerical techniques were explored as well (Rabczuk and Belytschko 2006). However, a great majority of these studies on concrete has not been introduced in practical calculations of real engineering structures. Engineers and researchers working on the design aspects of structural engineering, not directly involved in research on modeling and analysis of concrete structures, must rely on commercially available software and models implemented there in their work. Therefore, the experience gained on analysis of highly nonlinear structural engineering problems using commercially available finite element software, ABAQUS (SIMULIA 2008) will be discussed in this paper.

ABAQUS offers two solution techniques for such highly nonlinear problems. ABAQUS/Standard solves a system of nonlinear static equations iteratively to provide the solution of a problem at each load increment whereas ABAQUS/Explicit solves equations of motion by stepping forward in time and using very small increments without solving a system of algebraic equations at each increment. Both solution procedures in ABAQUS support the concrete damage-plasticity model which incorporates most of the concrete properties such as cracking, strain softening in tension, dilation, damage, compression hardening, stiffness degradation, etc.

The explicit dynamic solution procedure provided in ABAQUS/Explicit is generally used to solve dynamic problems. However, a static solution can also be obtained by using this procedure provided that the loading rate is very slow (the time within which the finite level of load is achieved is large) to minimize inertial effects in the structure. To achieve that goal, the maximum load should be reached within no less than about 10 to 50 times of the longest natural vibration period of the structure (Simulia 2008). The analysis of metal forming process is a good example for the application of the explicit solution procedure to static problems (Wagoner and Chenot 2005). Such analysis method, the so-called quasi-static analysis, is also very useful for solving highly nonlinear problems such as those resulting from sudden stiffness reductions due to concrete cracking in tension, for which tracing the descending (unstable) part of the equilibrium path is challenging. The challenge is due to the fact that the peak load is not known and that the final value of the monotonically increasing load is generally either smaller or larger than that peak value. In the first case, the unstable (descending) part of the load-displacement curve is not reached whereas in the second case large imbalance between the load and internal forces results in dynamic response in which inertia forces are not negligible.

The arc-length method or Modified Riks method (Riks 1979, Crisfield 1981), available in ABAQUS/Standard, is an alternative method that can be used to solve static nonlinear problems.

The arc-length method can efficiently capture geometric and material nonlinearity including the post-cracking response of concrete. The peak load, which is often the most important result for engineering purposes, can be determined using both arc-length and dynamic explicit methods. It is the purpose of this work to evaluate advantages and disadvantages of these two approaches in determining the response of the prestressed concrete members.

This work illustrates that the arc-length method (at least as implemented in ABAQUS/Standard) experiences convergence problems in solution for some combinations of concrete material properties and mesh configurations. The explicit dynamic method in ABAQUS/Explicit overcomes such numerical problems in the solution due to stabilizing effects of inertia. However, the time increment used in the explicit method has to be very small and the loading rate must be sufficiently low to make inertia negligible. Thus, the overall computational effort of the explicit dynamic procedure can be quite significant. Furthermore, as discussed subsequently, prestressing forces cannot be treated in the same manner with arc-length and explicit dynamic methods. In the explicit dynamic method, prestressing forces must also be introduced to the system slowly to prevent dynamic effects which creates the need for an additional quasi-static analysis before application of the load.

The fundamental advantages and disadvantages of the arc-length and explicit dynamic analysis are well known (Bathe 1996, Sun *et al.* 2000), but the manner in which they are manifested in the analysis of nonlinear problems typical for prestressed concrete structures does not appear to be documented. Considerable research has been devoted to the use of explicit solution method for the random vibration analysis of linear structures (Chang 2014, Su and Xu 2014). Sun *et al.* (2000) compared the performance of implicit and explicit methods for several dynamic problems including the impact of an elastic bar and a cylindrical disk on a rigid wall. The study showed that the cost of the explicit method is much higher than that of the implicit method for quasi-static problems. Nonlinear finite element analysis of prestressed concrete members has been reported by many researchers (Kawakami and Ito 2003, Kennedy and Abdalla 1992, Abdalla and Kennedy 1995, Broo *et al.* 2005). However, no information has been found in the literature that would advocate use of one method over the other in the analysis of prestressed concrete structures. Thus, in this study, the arc-length and explicit dynamic solution procedures were compared for the nonlinear finite element analysis of prestressed concrete members under monotonically increasing loads in order to evaluate the efficiency of these methods. Efficiency here includes not only computational effort but also quality of the results obtained which is assessed by comparing with available experimental results. To this end, a three-dimensional finite element model of an L-shaped, prestressed concrete spandrel beam was generated and analyzed with arc-length and explicit dynamic solution procedures in order to gain a better understanding of the overall advantages and disadvantages of these procedures.

2. General aspects of finite element modeling of prestressed concrete members

In three-dimensional applications of finite element analysis, concrete is usually modeled using eight-node brick elements with reduced integrations. The element library of ABAQUS/Explicit for brick elements is limited to eight-node brick elements with reduced integrations whereas ABAQUS/Standard supports both eight- and twenty-node elements. Conventional reinforcement is represented by truss elements, which carry axial load only. Therefore, a uniaxial stress-strain relationship such as the elastic-plastic material idealization is sufficient to define the behavior of

reinforcement. Using the embedded element option in ABAQUS, an assembly of reinforcement (i.e., embedded element) is located in the concrete solid (i.e., host element). In this case, translational degrees of freedom at a node of a reinforcing bar are constrained by the corresponding degrees of freedom in the concrete solid. This approach assumes that there is perfect bonding between rebar and concrete interfaces. However, this method neglects the load transfer in the cracked concrete element around the rebar. The behavior of cracked, reinforced concrete element is generally represented by introducing an additional ductility to the post-peak branch of concrete model in tension, the so-called “tension stiffening” effect.

Prestressing strands are also modeled using truss elements embedded in the concrete solid and perfect bond between concrete/strand interfaces. A proper model for the transfer length of strands becomes essential in the analysis of prestressed concrete beams, otherwise the beam fails in the end regions where the stress level in the concrete can be very high, depending upon the transfer of prestressing force. The simplest modeling approach is to divide the transfer length of a strand into a number of segments and gradually decrease the cross sectional area of each segment to the beam ends (Hassan *et al.* 2007). When the prestressing force is defined as a constant initial stress along a strand, a strand segment with reduced cross sectional area will be subjected to lower prestressing force and hence lower stresses are transferred to the concrete.

3. Arc-length method

The arc-length method is a static solution procedure that allows evaluation of the load-deflection path for a nonlinear structural response including descending branches. The method can efficiently account for material and geometric nonlinearity. Unlike the force-control approach, in which the magnitude of the load is specified, or the displacement control approach, in which the magnitude of a selected displacement is specified and the corresponding load magnitude computed, the arc-length method does not require specification of either. Instead, as shown in Fig. 1, the advancement from point $n-1$ to point n on the equilibrium path (specified by unknown values of the displacement and force) is achieved by the definition of the distance l_n between these two points.

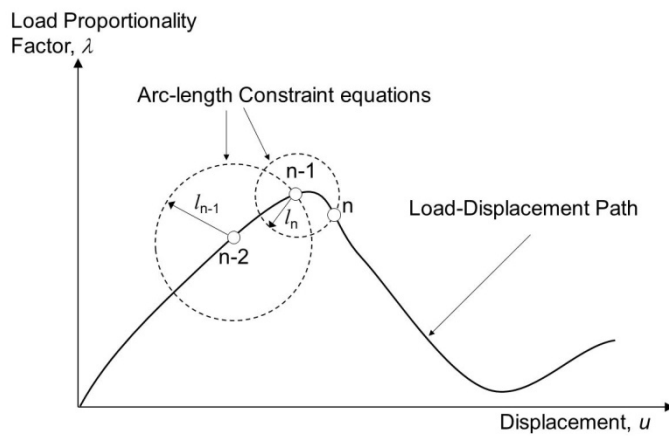


Fig. 1 Arc-length procedure

To this end, in addition to the governing equation, a constraint equation, as given in Eq. (1), is necessary for the solution of the simultaneous equations governing the problem in which the load proportionality factor, λ , is an additional unknown. The constraint equation describes the arc length (l_n) of the load-displacement path.

$$\lambda = \pm \sqrt{l^2 - \Delta u^2} \quad (1)$$

The load magnitude P_{total} at the new point on the equilibrium path is defined as:

$$P_{total} = \lambda P_{ref} \quad (2)$$

where P_{ref} is the reference load vector and λ is the load proportionality factor, which is an unknown representing the load. Nonlinear equilibrium equations are solved together with the constraint equation using Newton's method defining one arc-length step. The result is the nodal displacement vector, u and the load proportionality factor, λ .

4. Explicit dynamic method

The static response of a prestressed concrete beam can also be investigated by using the explicit dynamic procedure. For the static solution of the problem, inertial effects produced by the structural mass should be minimized in explicit dynamic analysis. By either increasing the mass density of concrete or decreasing loading rate, the oscillation of the beam can be limited and inertial forces made negligible (Fig. 2). In practice, if the loading period T over which the load is increased to its final value, is sufficiently larger than the longest natural period of the structure, the inertial effect is usually negligible. The figure also illustrates that dynamic response initiates when the load reaches a local maximum in the static equilibrium path. Therefore, the descending part of that path cannot be traced using dynamic explicit method as it requires some sort of displacement control (enforced in the arc-length approach) to reach a static equilibrium. However, one can still determine the peak load using the explicit dynamic approach.

The time increment, Δt , used in the explicit dynamic analysis is automatically determined by the numerical stability limit of the explicit method implementation used in ABAQUS. There is a close relationship between the stability limit and the time required for a stress wave to cross the

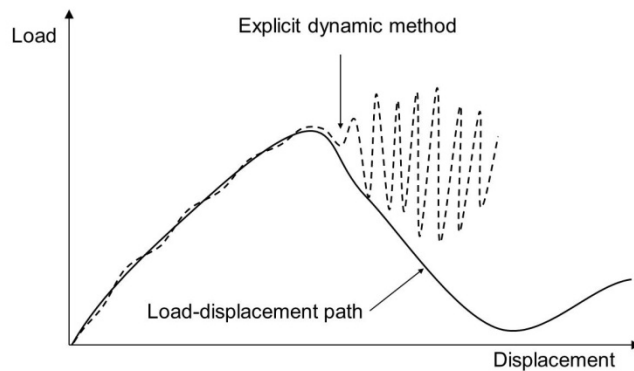


Fig. 2 Explicit dynamic procedure

smallest element dimension in the model. When the model consists of elements with very small dimensions, a small time increment has to be used and total computational effort will increase, given a fixed loading period, T . The number of load increments, m , required to complete the analysis is $m=T/\Delta t$. Computational effort for the explicit dynamic analysis is proportional to the product of the number of time increments, m , and the total number of degrees of freedom.

An optimum value for the loading period, T , can be easily found if the longest period of natural vibration, T_n , is known (or estimated). As a starting point, the explicit dynamic analysis has been performed here for a loading period, T , which is a value in the range of ten to fifty times larger than that period of the lowest frequency of vibration, T_n (i.e., $T=10T_n$ to $50T_n$) (Simulia 2008). For such a loading period, inertial effects are generally negligible, but computational effort might be high. In the subsequent analyses, the loading period has been gradually reduced until a significant variation due to inertia is observed in the analysis results. The magnitude of inertial forces can be evaluated by monitoring the ratio of kinetic energy to total strain energy during the analysis. When that ratio is less than 0.5 percent, the resulting response has been found to be essentially quasi-static (Sun *et al.* 1999, Malm and Holmgren 2008).

Furthermore, the natural period does not remain constant during the analysis and increases when the structural stiffness reduces due to concrete cracking or steel yielding. Therefore, the loading period initially determined based on the fundamental period of the elastic structure is likely to be inadequate to ensure that inertial effects are minimized for the entire duration of analysis.

5. Modeling of prestressing force

Concrete cracking reduces both torsional and flexural stiffness of prestressed concrete beam and causes significant increase in deflections. However, prestressing forces delay cracking under flexure. Therefore, prestressing strands should be modeled properly in order to capture concrete cracking at the appropriate load level, as well as the corresponding deflection of the beam with sufficient accuracy. A significant modeling aspect of prestressed concrete beams is to define appropriately the initial stress state due to prestressing at the beginning of the analysis. Using the arc-length method in ABAQUS/Standard, the prestressing force in a strand can be defined as an initial stress that is assumed to be constant along the truss element of the strand in the model. Then, in the first increment of the arc-length analysis, the structure will reach the equilibrium state for this initial stress condition. If the same modeling approach for prestressing forces is applied in the explicit dynamic procedure, the initial stress state creates an impact loading in the beam and the transient response includes oscillations with amplitudes that can be large. Therefore, prestressing forces in the explicit dynamic analysis must be modeled in an alternate manner, utilizing either a direct or an indirect procedure.

In the direct modeling approach, the geometry and material states of the beam, when subjected to prestressing effects only, are obtained using the static analysis procedure in ABAQUS/Standard and transferred to ABAQUS/Explicit as an initial condition. Since the beam is already in equilibrium at the end of the static analysis, the initial condition defined at the beginning of the explicit dynamic analysis does not lead to impact loading. However, ABAQUS/Standard and ABAQUS/Explicit process data in different ways and the forces transferred from ABAQUS/Standard may not be in perfect equilibrium in ABAQUS/Explicit, which causes minor oscillation of the beam. These oscillations, however, will become negligible in the rest of the

explicit analysis.

In the indirect modeling approach, the prestressing force in a strand is introduced via an artificial reduction in strand temperature. Without transferring any data from ABAQUS/Standard to ABAQUS/Explicit, the response of prestressed concrete beam is evaluated with two consecutive explicit analyses. In the initial analysis, a temperature change is slowly applied to the prestressing strands to generate the intended prestressing effect, after which the temperature remains constant and the second explicit analysis is conducted to determine the beam response to the desired load. It should be noted that temperature change does not affect the physical properties of concrete or steel in ABAQUS, and it is used solely as a way to create the desired initial stresses in the strands. The required temperature change, ΔU_{st} , can be obtained using Eq. (3), in which α_{st} represents the thermal expansion of the strand, E_{st} is the elastic modulus of strands and f_{pe} is the effective prestress after losses.

$$\alpha_{st} \Delta U_{st} = f_{pe} / E_{st} \quad (3)$$

6. Modeling of concrete

Concrete is an inhomogeneous material and exhibits properties that vary broadly from one analysis to another. The stress-strain relation of concrete in compression has a nonlinear ascending branch up to ultimate strength, followed by a strain softening region. Concrete in tension, however, cracks at very low stress levels. The behavior of concrete under multi-axial stress states is even more complex. Consequently, defining a material model for concrete that represents its response with a high level of fidelity is a very challenging task (Chen 1982, Kwak and Filippou 1990). The concrete damage plasticity model available in ABAQUS is used in this study for both the arc-length and the explicit dynamic analyses because it is the only concrete model offered in both ABAQUS/Standard and ABAQUS/Explicit. In a previous study (Mercan *et al.* 2010), this model was shown to offer the flexibility needed to represent various properties of concrete. The concrete damage-plasticity model in ABAQUS relies on the methodology proposed by Lubliner *et al.* (1989) for monotonic (i.e. unidirectional) loading and by Lee and Fenves (1998a, b) for cyclic loading. The concrete damage-plasticity model brings together isotropic damage elasticity and non-associated multi-hardening plasticity. The concrete damage-plasticity model assumes two failure modes; cracking in tension and crushing in compression.

In general, the resistance of cracked concrete is often ignored in design for simplicity. However, neglecting the post-cracking behavior of concrete may lead to significant error in the nonlinear finite element analysis of prestressed concrete structures. The post-cracking response of concrete plays an important role in deflections, crack width, bond-slip, and shear transfer etc. (Gopalaratnam and Shah 1985). Cracking initiates once the stress level at an integration point in a concrete element reaches the concrete tensile strength. Cracking introduces gradual strength decrease at this integration point in accordance with the post-peak response of concrete model in tension. However, the cracked reinforced concrete element can still transfer load through the rebar as full kinematic compatibility between concrete and rebar has been enforced in the model used in this study. Effects such as bond-slip, present in real rebar-concrete interactions, are approximated in the concrete model by modifying the tension softening region relative to that for plain concrete as shown in Fig. 3, the so-called “tension stiffening” behavior (Nayal and Rasheed 2006).

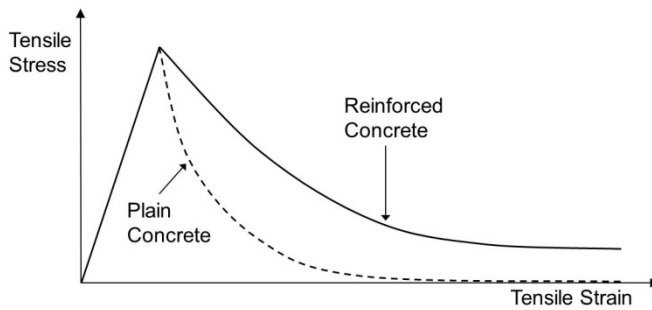


Fig. 3 Tension stiffening of concrete due to concrete-rebar interaction

Defining proper tension stiffening behavior plays an essential role in the quality of the results and the performance of the algorithm used. Numerical solution of a model generated with ABAQUS/Standard might be unstable if too small amount of tension stiffening effect is introduced into the concrete model. It is commonly suggested that numerical stability can be achieved for the solution of an arc-length analysis when the ultimate tensile strain of concrete, including the effect of tension stiffening, is equal to a value ten times larger than that of plain concrete (Simulia 2008). However, due to stabilizing effect of inertia, the explicit dynamic procedure does not experience numerical instability even if the post-cracking response of plain concrete is used in the concrete model and tension stiffening effect is ignored.

The post-peak response of concrete in tension can be defined using fracture energy, G_f , which is a material property indicating the energy required to open a unit area of crack in a plain concrete specimen (Hillerborg *et al.* 1976, Marzouk and Chen 1995). The fracture energy, which is equal to the area under tensile stress – opening displacement curve, $\sigma_t(w)$, can be approximately calculated using Eq. (4) where f_t is the tensile strength of concrete and w_t is the total cracking displacement. In this equation, a linearly descending post-cracking regime for concrete in tension is assumed. The tension stiffening effect (i.e., the interaction between cracked concrete and steel) is generally taken into account by using a fracture energy value for reinforced concrete, which is larger than that for plain concrete.

$$G_f = \int \sigma_t(w) dw \approx \frac{f_t w_t}{2} \quad (4)$$

7. Modeling of an L-Shaped, precast, prestressed concrete spandrel beam

The relative merits of the arc-length and explicit dynamic methods were demonstrated by evaluating the response of an L-shaped, prestressed concrete spandrel beam under monotonically increasing loads. Such beams were suited for this study since they exhibit a complex structural response to loading and thus constitute a good test for various aspects of the model. There is also a practical reason for this choice as the spandrel beams have been widely used in the perimeter of precast concrete frames. They support deck beams and are connected to column corbels at their ends. The cross section of an L-shaped spandrel beam is under the combined effects of shear, torsion and bending, as shown in Fig. 4. The vertical loads acting on the beam ledge create biaxial

bending due to the asymmetric shape of the cross section. The eccentricity of the vertical loads also causes a torsional effect, which leads to twisting of the member. Prestressing forces further complicate the behavior of a spandrel beam.

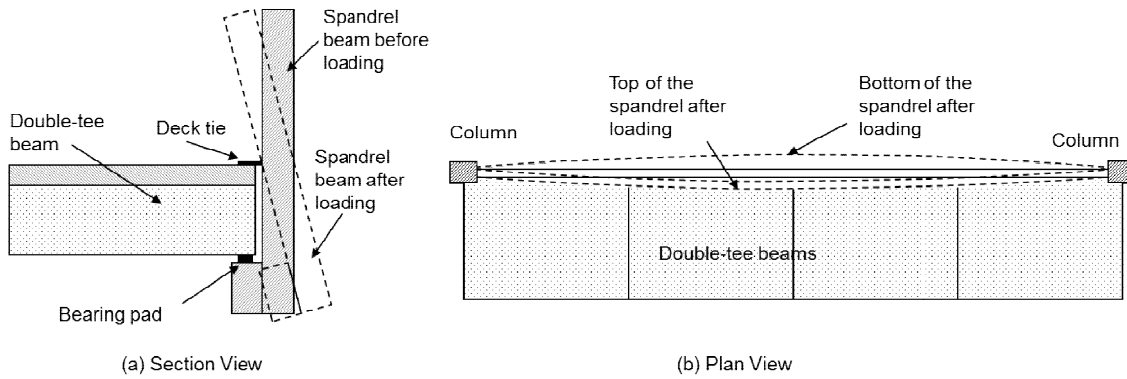


Fig. 4 L-shaped spandrel beam before and after loading



Fig. 5 Spandrel beam configuration (all dimensions are in mm)

7.1 Description of the experiment

An experimental study of full-size, L-shaped, prestressed concrete spandrel beams was selected from the literature (Lucier *et al.* 2007). The spandrel specimen, as shown in Fig. 5, had a length of 13.7 m (45 ft) and a web with a depth of 1.5 m (5 ft) and width of 0.2 m (8 in). The ledge of the spandrel was 0.2 m by 0.2 m (8 in by 8 in) section and terminated at a 0.3 m (12 in) distance from both ends of the spandrel. The prestressing strands were low relaxation, 1860 MPa (270 ksi), 12.7 mm ($\frac{1}{2}$ in) diameter seven-wire steel strands with initial prestressing forces of 100 kN (22.5 kips) for Type A and 68.5 kN (15.4 kips) for Type B, as shown in Fig. 6. The cylinder strength for concrete in compression was measured as 49.6 MPa (7,190 psi). A 152×152 mm (6×6 in)-W4×W4 mesh of welded wire fabric was placed on both sides of the spandrel web. More details related to the reinforcement assembly can be found in Lucier *et al.* (2007).

In the test set-up, both ends of the spandrel beam rested on teflon-coated bearing pads with reduced friction and were laterally supported with 25 mm (1 in) diameter tie-back bolts. The

specimen was also laterally supported within the span at the mid-height elevation by means of deck-ties, connecting the spandrel to 3 m (10 ft) wide double-tee deck beams. The spandrel ledge supported these double-tee deck beams on which hydraulic jacks were attached.

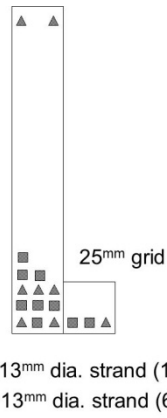


Fig. 6 Prestressing strand details

Due to the self-weight of the spandrel specimen and testing equipment, the vertical reaction force of 98 kN (22 kips) was measured at the bearing support. Three load levels: service (dead + live), service with snow (dead + live + snow) and fully factored (1.2 dead + 1.6 live + 0.5 snow), were considered for the spandrel supporting an 18.3-m (60-ft) span double-tee. The load was increased until each of these load levels was reached and then released. Finally, the spandrel was loaded up to failure. During the experiment, the vertical and lateral displacements at the top and bottom of the spandrel mid-span, and the rotation of the spandrel quarter-span and the vertical reaction at the end support were monitored.

7.2 Description of the finite element model

The spandrel beam test specimen described above was modeled in ABAQUS. Due to the symmetry of the spandrel geometry and loading with respect to the mid-span, only one-half of the spandrel was modeled and symmetry boundary conditions were applied to the mid-span cross section. In the test setup, the bearing pad at the end support was in contact with 0.3 m by 0.2 m (12 in by 8 in) surface area at the bottom of the spandrel web. This surface was forced to remain plane in the model by defining planar constraint equations and a single point in the middle of this surface was fixed against vertical translation. Such modeling technique eliminates singularity problems and bypasses a need for much more complex contact analysis.

The tie-back bolts were modeled using linear spring elements with the stiffness of 100 kN/mm (570 k/in), assumed to be equal to the axial stiffness of a 1-m long bolt with the diameter of 25 mm (1 in). The deck ties made of 76mm×152mm×9.5mm (3in×6in×3/8in) steel plates were also modeled using spring elements at the mid-height elevation of the front face of the spandrel web. For each deck tie, two linear spring elements with the stiffness of 1,910 kN/mm (10,900 k/in) per spring were defined in order to accommodate the finite size of the connections.

The concrete solid of the spandrel was modeled using 8-node brick elements with reduced integration and hourglass control. The concrete solid was analyzed for three different mesh configurations; coarse, intermediate, and fine with the average element size of 203 mm (8 in), 102 mm (4 in), and 51 mm (2 in), respectively. The elastic modulus of concrete was calculated as 33 GPa (4,800 ksi) for the compressive strength of 49.6 MPa (7,190 psi), using the elastic modulus equation given the ACI Committee 318 building code document (2011). The uniaxial stress-strain relation of concrete under compression is assumed as shown in Fig. 7. Post-peak behavior of concrete in tension was defined using a concrete fracture energy of 1.75 kN/m (0.01 kips/in) and a tensile strength of 3.5 MPa (0.509 ksi).

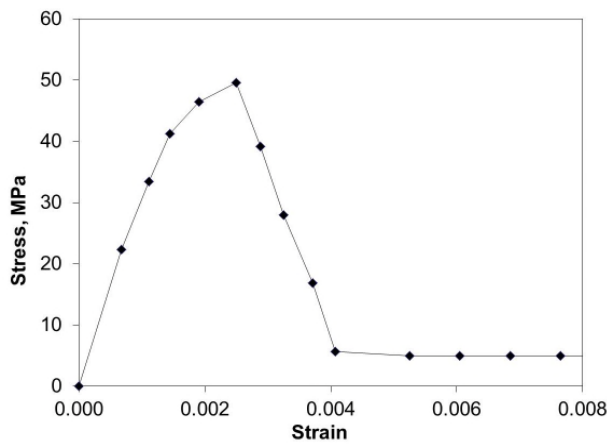


Fig. 7 Uniaxial stress-strain relation for plain concrete in compression

The steel reinforcement assembly, welded wire mesh and prestressing strands were modeled using linear truss elements with a typical element size of 50 mm (2 in). Elastic-perfectly plastic material behavior was assumed for all steel elements with the elastic modulus of 200 GPa (29,000 ksi). The yield strengths for mild steel, welded-wire-mesh reinforcement and prestressing strands were taken as 445 MPa (64.5 ksi), 675 MPa (98 ksi), and 1,675 MPa (243 ksi), respectively. A transfer length of 510 mm (20 in) was modeled by gradually reducing the cross section of the strand at one end. The loss in the initial prestress forces was assumed as 15% excluding the effect of elastic shortening of concrete (Hassan 2007). Thus, the effective prestressing forces of 85 kN (19.1 kips) for Type A strands and 57.8 kN (13.1 kips) for Type B strands were considered in the model.

Before the analysis of the spandrel model with the arc-length solution approach, the model was first analyzed with load-controlled static procedure to determine the state of strains and stresses in the beam due to its self-weight and prestressing forces. Stresses in strands after losses were introduced as an initial stress state. At the end of this preliminary static analysis, the reaction force at the support was obtained as 100 kN (22 kips). Next, the spandrel model was analyzed using arc-length procedure for which the double-tee loads acting on the spandrel ledge were controlled at each analysis step. The initial arc length increment was taken quite large (e.g., 0.01 out of a total arc length of 1.0) since severe nonlinearity was not expected in the solution for low load levels.

This allowed for a faster advancement along the equilibrium path at early stages of loading.

The subsequent arc length increments were automatically determined by ABAQUS, based on the number of iterations needed to converge.

The explicit dynamic approach also requires an initial analysis stage for defining prestressing effects in the model. These prestressing forces were introduced with artificial temperature changes in strands. For each strand type (i.e. Type A or Type B) a different temperature change was defined to achieve the required prestressing force after losses. After this initial prestressing analysis stage, the spandrel beam model was analyzed using explicit dynamic analysis for which the double-tee loads were increased at each time step.

7.3 Loading rate in explicit dynamic analysis

During the explicit dynamic simulation, the inertial effects must be minimal in order to obtain the static response of the spandrel beam. The magnitude of the inertial effects highly depends on the loading rate used in the analysis. The loading rate should be selected in such a way that the finite load level is reached within 10 to 50 times of the fundamental period, T_n , of the structure. For this reason, the modal analysis of the spandrel model was performed and resulted in the fundamental period of 0.075 sec. Thus, the finite load level should be achieved between the loading periods of 0.75 sec and 3.75 sec (i.e., $10T_n$ and $50T_n$). This is obviously a rule of thumb estimate as the real rate of loading depends also on the level of the final load to be applied. Nevertheless, it has been used here as a guide.

The sensitivity of the explicit dynamic analysis results to loading period was investigated. Three different loading periods; 1 sec, 0.5 sec and 0.25 sec, were analyzed with intermediate mesh configuration. The analysis results, as shown in Fig. 8, were plotted against the test results in terms of support reaction vs lateral deflections at the top and bottom of the spandrel mid-span. The displacements toward the inner face of the spandrel (the face that is connected to the double-tee beams) were assumed positive. The top of the spandrel web moved inward at the mid-span and had positive displacements whereas the bottom of the spandrel moved outward. The support reaction in the figure began with zero value as the self-weight of the specimen (100 kN) were excluded from the support reaction.

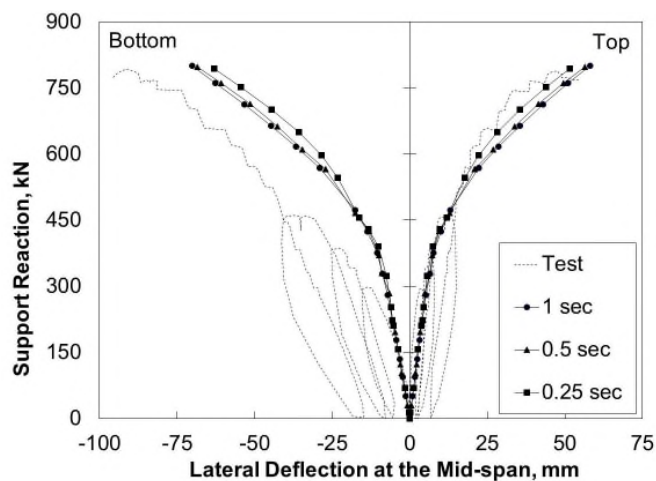


Fig. 8 The effect of loading period on explicit dynamic analysis results

All three loading periods yielded the similar results for the support reactions up to 400 kN (90 kips), for which the spandrel concrete cracking initiated. For support reactions greater than 400 kN (90 kips), spandrel stiffness reduced due to concrete cracking and hence larger lateral displacements occurred. Loading periods of 0.5 sec and 1 sec yielded similar spandrel response, indicating inertial effects are minimal for both loading periods. However, for 0.25 sec loading period, the spandrel model exhibited stiffer response in the inelastic region which can be attributed to dynamic effects. After concrete cracking, the stiffness of the spandrel decreased and the natural period of vibration increased. Thus, the minimum loading period leading to the quasi-static response also increased and the loading period of 0.25 sec became inadequate to prevent dynamic effects in the inelastic region.

Another and perhaps more meaningful way to evaluate the magnitude of dynamic effects is to check the maximum ratio of kinetic energy to strain energy during the analysis. The energy ratios for different loading periods and mesh configurations are shown in Fig. 9. For 0.25 sec loading period, the maximum energy ratio was greater than the limit of 0.5 percent, which supports the finding, discussed earlier, that the dynamic effects were significant in this case. As shown in Fig. 9, the loading period of 0.5 sec had the maximum energy ratio of 0.5 percent and was the minimum allowable loading period to ensure negligible dynamic effects.

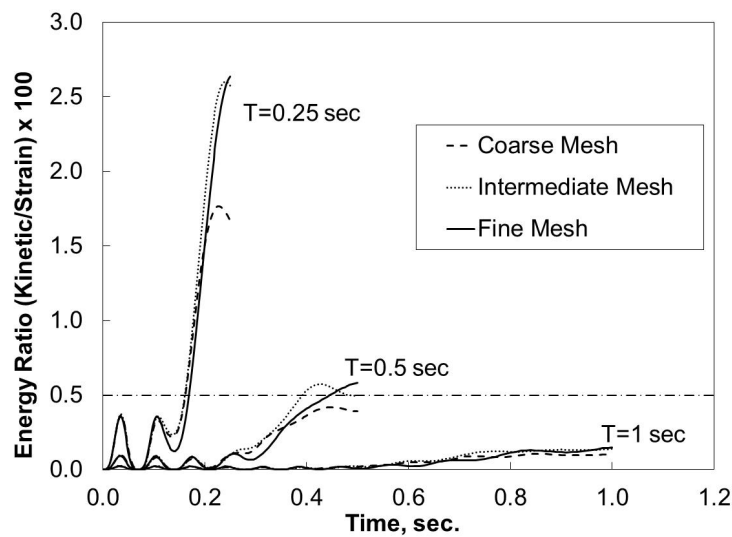


Fig. 9 Energy ratios for different loading periods and mesh configurations

8. Comparison of the solution procedures for the spandrel beam example

8.1 Mesh configuration

The robustness of the arc-length and explicit dynamic procedures was assessed for fine, intermediate and coarse mesh configurations. For the fine mesh configuration with the maximum element size of 51 mm (2 inches), the arc-length method failed to converge on the solution while the explicit dynamic method performed well, as shown in Fig. 10.

The arc-length analysis resulted in a severely nonlinear zone around the region where the tie-back springs were located. The horizontal reaction force in the spring can be large and the element in the concrete solid, associated with this reaction force, experienced large inelastic deformations. It should be noted that such localized inelastic deformations had not been observed for the arc-length analyses with coarse and intermediate meshes as the tie-back forces were distributed over a larger volume of solid concrete elements. Consequently, the arc-length method failed to converge on the solution for the fine mesh. However, the explicit dynamic method overcame such mesh-related problems. The loading period of 1 sec was used to minimize the dynamic effects in the simulation, as noted in the preceding section. Even though large inelastic deformations still appeared around the tie-back springs, the explicit dynamic algorithm effectively found the solution to this highly nonlinear problem.

The failure of the arc length method to converge is to be expected when the equilibrium path is not smooth. The calculations with this method require the tangent stiffness matrix of the system, which does not exist at some points if the equilibrium path is not smooth. This is likely to happen in the analysis of problems involving concrete whose constitutive equation has a sudden change due to cracking in tension, as shown in Fig. 3. When the stress field is complex (as in the case discussed in this study) and the elements are small enough that some of them do not contain any rebar, reaching a peak load in tension, and consequently encountering a point of a sharp turn on equilibrium path is particularly likely. This difficulty is, of course, inconsequential in explicit dynamic analysis in which case the tangent stiffness matrix is not used at all.

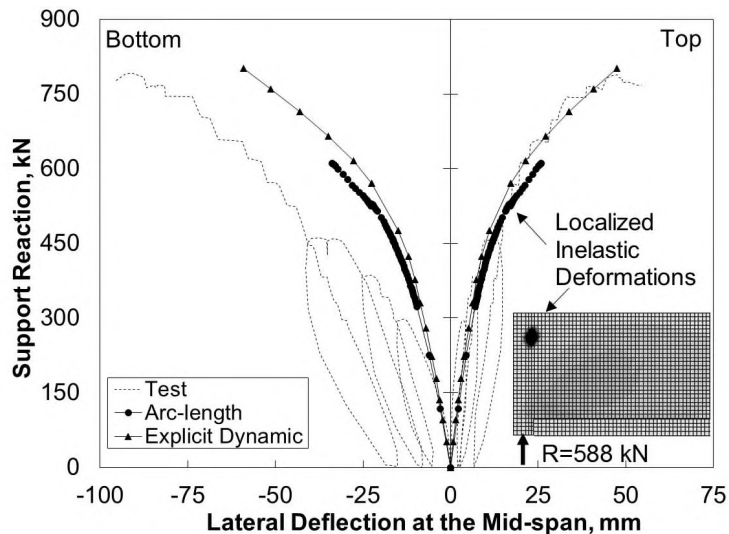


Fig. 10 Arc-length method vs. explicit dynamic method for fine mesh

8.2 Material model

The arc-length and explicit dynamic methods were also compared for different post cracking responses for concrete, i.e., tension stiffening magnitudes. As discussed above, the effect of tension stiffening can be introduced in the concrete model by using the fracture energy concept.

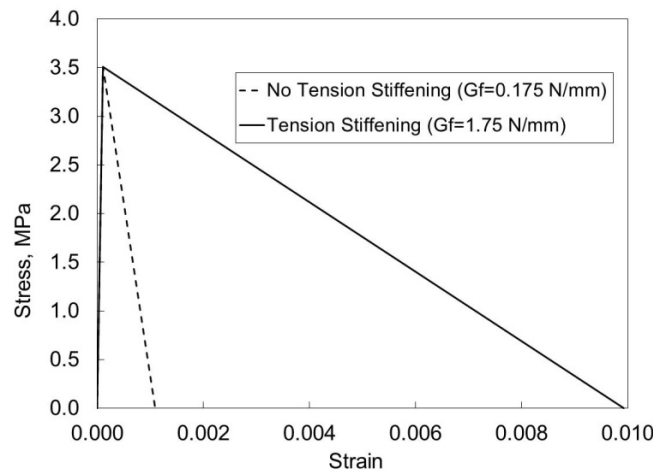


Fig. 11 Stress-strain relationships for concrete in tension

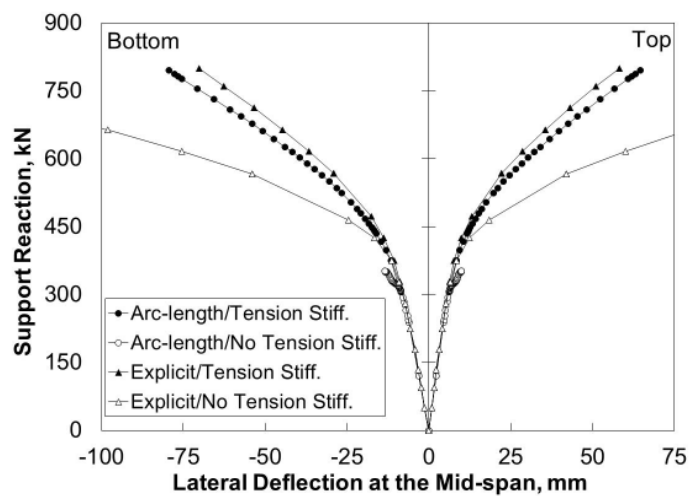


Fig. 12 The effect of tension stiffening

The fracture energy value of 1.750 N/mm (10 lbf/in) was used to represent the case with tension stiffening or reinforced concrete and the value of 0.175 N/mm (1 lbf/in) was used for virtually no tension stiffening or plain concrete. These fracture energy values were determined using equation (4) and the stress-strain relationships for concrete in tension as shown in Fig. 11. The tension stiffening effect for reinforced concrete was introduced into the model, as discussed in Section 6, by assuming the ultimate tensile strain of 0.1 mm/mm for reinforced concrete, which is larger than that of plain concrete by a factor of 10 (Simulia 2008). The opening displacement was assumed to be equal to the maximum element size used in the model. In this case it was 102 mm (4 in) as the intermediate mesh was considered. In Fig. 11, the strain softening region of the plain concrete was steeper than that for reinforced concrete, which was likely to make it harder for the arc-length method to achieve convergence in the former.

The results from the explicit dynamic and arc-length analyses with and without tension

stiffening effects are shown in Fig. 12. Both the arc-length and the explicit dynamic methods provided numerical solutions when the tension stiffening effect was included in the concrete model. However, the arc-length analysis without the effect of tension stiffening could not converge on the solution and failed right after concrete cracking initiated in the spandrel while the explicit dynamic procedure continued without interruption.

The tension stiffening effect for the concrete is closely related to the amount of steel distributed along the member. Therefore, it is not appropriate to ignore the tension stiffening for the spandrel beam since the steel ratio for a typical prestressed concrete spandrel beam is relatively high. However, this effect may pose problems for the analysis of lightly reinforced concrete beams for which tension stiffening is small.

8.3 Computational accuracy

The arc length and explicit dynamic methods, even though successfully providing a solution, exhibited small discrepancies in the load-deflection results due to several reasons. First, the comparison of a truly static solution with a dynamic solution with slowly increasing load always show some discrepancy as they are based on different sets of equations. Such discrepancy exists even if both solutions are perfectly accurate. Second, both the arc length method and any possible method for the dynamic analysis involve additional numerical errors which may superimpose, leading to a more pronounced discrepancy between static and dynamic analysis of essentially static problems. The explicit dynamic approach although considered efficient in the analysis of problems with complex material behavior, is also known as a method in which control of error can be limited. It may be achieved only by reducing the time step. As a result dynamic solution of a static problem using explicit approach may deviate from the static solution more than the solution using other dynamic solution algorithms (implicit).

In order to evaluate the accuracy of the arc-length and explicit dynamic methods for the spandrel beam example, the quarter-span rotations obtained using these methods were compared with experimental results, as shown in Fig. 13. The results were presented for all mesh configurations even though the arc-length method could not converge on a solution for the fine

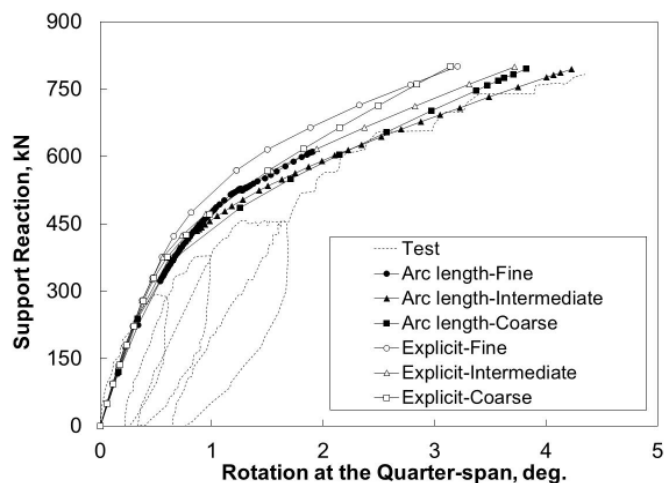


Fig. 13 Effect of analysis methods and mesh configurations

mesh. Explicit dynamic analyses were performed for a loading period of 1 sec. The arc-length method, if converging to a solution, generally provided the load-rotation results closer to the test measurements than the explicit dynamic method. The results of the explicit dynamic analysis were more sensitive to the mesh refinement than those of the arc-length method. Mesh refinement from coarse mesh to intermediate mesh configuration had a minor effect in the results of the arc-length analysis. However, from the practical viewpoint, one can say that all of the simulations in Fig. 13 provided comparable approximations of the experimental results.

8.4 Computational effort

The effectiveness of the solution methods can also be evaluated in terms of computational effort required to reach a solution for the spandrel beam example considered here. The computational effort or CPU (process) time generally depends on the solution approach and the size of the problem. Thus, CPU time consumed by these two solution methods was compared for different mesh configurations. The coarse, intermediate, and fine mesh models included 754, 2,504, and 18,928 solid concrete elements, respectively. For the explicit dynamic analysis, three loading periods, 2 sec, 1 sec, and 0.5 sec, were also considered. CPU time spent by the initial analysis for prestressing and self-weight loads was excluded. The analyses were performed with IBM BladeCenter Linux Cluster with AMD Opteron 2218 processors.

The arc-length procedure used less CPU time than the explicit method for coarse and intermediate mesh configurations, as shown in Fig. 14. However, the fine mesh had no basis for comparison as the arc length method did not converge on any solution. When the number of solid elements increased approximately threefold by changing the mesh configuration from coarse to intermediate, CPU time increased by a factor of 3 for the arc-length procedure and a factor of 1.5 for the explicit dynamic procedure. Additionally, from intermediate to fine mesh, the number of elements increased by a factor of 8, but CPU time increased only by a factor of 5 for explicit dynamic procedure. Also, for loading periods used in the explicit dynamic method, the factors of

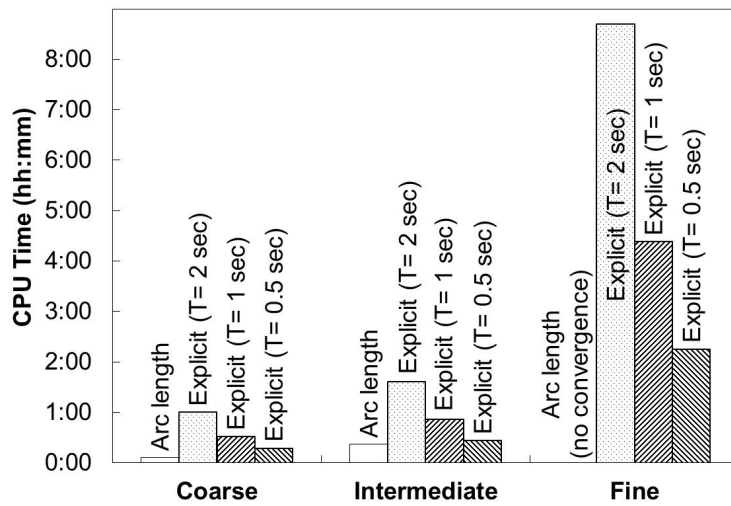


Fig. 14 Comparison for process (CPU) time

increase on CPU time due to mesh refinement were similar.

Consequently, the arc-length method required less process time than the explicit dynamic method for the spandrel beam example considered here. However, the process time for the explicit dynamic procedure was much less sensitive to the change of the problem size than that of the arc length method. In other words, for very large problems, the explicit dynamic procedure can be more process time efficient.

9. Conclusions

In this study, the advantages and disadvantages of the arc-length and explicit dynamic finite element approaches were investigated in the context of strongly nonlinear structural response. Therefore, the three-dimensional, non-linear finite element analysis of an L-shaped, prestressed concrete spandrel beam under monotonically and quasi-statically increasing loads was considered as a model problem in this work.

The analysis results showed that the arc-length approach fails while the explicit dynamic method still yields a solution when (a) the effect of tension stiffening for concrete is small and (b) the mesh configuration is refined. The small value for tension stiffening corresponds to a steep change in the response of concrete in tension due to cracking. The mesh refinement generates more concrete elements within a region surrounded by steel rebar. These concrete elements are more prone to localized inelastic deformations as they are not engaged with steel reinforcement. Thus, in the analysis of lightly reinforced concrete structures, for which the tension stiffening for concrete is expected to be small, the arc-length method is likely to fail converge on a solution. When both methods yield solutions, those solutions are close to each other provided that prior to the explicit dynamic analysis of a static problem, the loading period over which the load is increased to its final value (the rate of loading) is determined so as to make the dynamic effects negligible. Also, even for the coarse mesh, the results of the arc-length method are in good agreement with the experimental results.

The explicit method requires somewhat more computational effort than the arc-length method. However, as indicated above, it is less sensitive to various model parameters and, consequently, more robust in the sense that it provides a solution in cases where the arc length method is likely to fail. The computational cost of the explicit method can be minimized by careful selection of the loading period over which the load is increased to its final value. In conclusion, a loading period (T) equal to fifty times the fundamental period (T_n) of a concrete structure is probably too long even assuming that when the stiffness of the structure decreases due to concrete cracking, the fundamental period of the structure increases and hence the influence of dynamic effects increases as well. However, since the spread of inelastic zones is somewhat different for different mesh configurations, the minimum loading period ensuring negligible dynamic effects depends to some extent on the mesh, even though the fundamental period of a linear-elastic structural model is virtually independent of the mesh configuration. The present investigation indicates that a loading period (T) equal about 10-15 times the fundamental period (T_n) is adequate.

Based on these findings, it may be concluded that from the viewpoint of computational efficiency, the arc-length method should be preferred over the explicit dynamic analysis for three-dimensional, nonlinear finite element analysis of prestressed concrete beams under monotonically increasing loads so long as convergence to a solution is achieved. There appears to be a strong correlation between loading period, fundamental period, and mesh size (element size).

Furthermore, unlike the explicit dynamic approach, the arc-length method allows the tracing of the complete equilibrium path, including any descending branches. However, the explicit dynamic analysis is a robust technique which is able to provide a solution in cases with a complex material behavior or a refined mesh when the arc-length method fails. It should be noted that for unreinforced, brittle materials some of these observations may apply, but the lack of reinforcement will also have an influence not investigated in this work. Therefore, the observations and recommendations are limited to reinforced or prestressed concrete.

References

- Abdalla, H. and Kennedy, J.B. (1995), "Dynamic analysis of prestressed concrete beams with openings", *J. Struct. Eng.*, **121**(7), 1058-1068.
- American Concrete Institute (ACI) Committee 318 (2011), "Building code requirements for structural concrete", Farmington Hills, Mich.
- Bathe, K.J. (1996), *Finite Element Procedures*, New Jersey, Prentice Hall.
- Belytschko, T., Organ, D. and Gerlach, C. (2000), "Element-free Galerkin methods for dynamic fracture in concrete", *Comput. Method. Appl. Mech. Eng.*, **187**(3-4), 385-399.
- Broo, H., Lundgren, K. and Engström, B. (2005), "Shear and torsion interaction in prestressed hollow core units", *Mag. Concrete Res.*, **57**(9), 521-533.
- Chang, S.Y. (2014), "Numerical dissipation for explicit, unconditionally stable time integration methods", *Earthq. Struct.*, **7**(2), 159-178.
- Chen, W.F (1982), *Plasticity in reinforced concrete*, McGraw-Hill, New York.
- Crisfield, M.A. (1981), "A fast incremental/iteration solution procedure that handles snap-through", *Comput. Struct.*, **13**, 55-62.
- Gopalaratnam, V.S. and Shah, S.P. (1985), "Softening response of plain concrete in direct tension", *American Concrete Institute J.*, **82**(3), 310-323.
- Grassl, P. and Jirásek, M. (2006), "Damage-plastic model for concrete failure", *Int. J. Solid. Struct.*, **43**(22-23), 7166-7196.
- Grassl, P. and Rempling, R. (2007), "Influence of volumetric-deviatoric coupling on crack prediction in concrete fracture tests", *Eng. Fract. Mech.*, **74**(10), 1683-1693.
- Hassan, T., Lucier, G., Rizkalla, S. and Zia, P. (2007), "Modeling of L-shaped, precast, prestressed concrete spandrels", *Precast/Prestressed Concrete Institute J.*, **52**(2), 78-92.
- Hillerborg, A., Moeder, M. and Peterson, P.E. (1976), "Analysis of crack formation and crack growth in concrete by means of fracture mechanics and finite element", *Cement Concrete Res.*, **6**(6), 773-792.
- Jirásek, M. and Grassl, P. (2008), "Evaluation of directional mesh bias in concrete fracture simulations using continuum damage models", *Eng. Fract. Mech.*, **75**(8), 1921-1943.
- Jirásek, M. and Marfia, S. (2005), "Non-local damage model based on displacement averaging", *Int. J. Numer. Method. Eng.*, **63**(1), 77-102.
- Kawakami, M. and Ito, T. (2003), "Nonlinear finite element analysis of prestressed concrete members using ADINA", *Comput. Struct.*, **81**, 727-734.
- Kennedy, J.B. and Abdalla, H. (1992), "Static response of prestressed girders with openings", *J. Struct. Eng.*, **118**(2), 488-504.
- Kwak, H.G. and Filippou, F.C. (1990), "Finite element analysis of reinforced concrete structures under monotonic loads", Department of Civil Eng., Univ. of California, Berkeley.
- Lee, J. and Fenves, G.L. (1998), "A plastic-damage model for cyclic loading of concrete structures", *J. Eng. Mech.*, **124**, 882-900.
- Lee, J. and Fenves, G.L. (1998), "A plastic-damage concrete model for earthquake analysis of dams", *Earthq. Eng. Struct. Dy.*, **27**, 937-956.

- Lubliner, J., Oliver, J., Oller, S. and Onate, E. (1989), "A plastic-damage model for concrete", *Int. J. Solid. Struct.*, **25**(3), 299-326.
- Lucier, G., Rizkalla, S., Zia, P. and Klein, G. (2007), "Precast concrete, L-shaped spandrels revisited: Full-scale tests", *Precast/Prestressed Concrete Institute J.*, **52**(2), 62-76.
- Malm, R. and Holmgren, J. (2008), "Cracking in deep beams owing to shear loading. Part 2: Non-linear analysis", *Mag. Concrete Res.*, **60**(5), 381-388.
- Marzouk, H. and Chen, Z.W. (1995), "Fracture energy and tension properties of high-strength concrete", *J. Mater. Civil Eng.*, **7**(2), 108-116.
- Mercan, B., Stolarski, H.K. and Schultz, A.E. (2010), "Finite element modeling of prestressed concrete spandrel beams", *Eng. Struct.*, **32**(9), 2804-2813.
- Nayal, R. and Rasheed, H.A. (2006), "Tension stiffening model for concrete beams reinforced with steel and FRP bars", *J. Mater. Civil Eng.*, **18**(6), 831-841.
- Prinja, N.K. and Shepherd, D. (2005), "Simulating structural collapse of a PWR containment", *Proceedings of the 17th International Conference on Structural Mechanics in Nuclear Engineering*, **235**, 2033-2043.
- Rabczuk, T. and Belytschko, T. (2006), "Application of particle methods to static fracture of reinforced concrete structures", *Int. J. Fract.*, **137**(1-4), 19-49.
- Riks, E. (1979), "An incremental approach to the solution of snapping and buckling problems", *Int. J. Solid. Struct.*, **15**, 529-551.
- SIMULIA (2008), *ABAQUS Analysis User's Manual*, Version 6.8. Dassault Systèmes Corp., Providence, RI.
- Sun, J.S., Lee, K.H. and Lee, H.P. (2000), "Comparison of implicit and explicit finite element methods for dynamic problems", *J. Mater. Process. Tech.*, **105**, 110-118.
- Thevendran, V., Chen, S., Shanmugam, N.E. and Richard Liew, J.Y. (1999), "Nonlinear analysis of steel-concrete composite beams curved in plan", *Finite Elem. Anal. Des.*, **32**, 125-139.
- Su, C. and Xu, R. (2014), "Random vibration analysis of structures by a time-domain explicit formulation method", *Struct. Eng. Mech.*, **52**(2), 239-260.
- Wagoner, R.H. and Chenot, J.L. (2005), *Metal forming analysis*, Cambridge University Press.

Notation

The following symbols are used in this paper

E_c	= elastic modulus of concrete;
E_{st}	= elastic modulus of strands;
f_{pe}	= effective prestress in strands;
f_t	= tensile strength of concrete;
G_f	= fracture energy for concrete;
l_n	= arc length;
m	= number of increments;
n	= a point on the equilibrium path;
P_{ref}	= reference load;
P_{total}	= total load;
T	= loading period;
T_n	= the longest period of natural vibration;
w	= opening displacement of concrete;
w_t	= total opening displacement of concrete;
Δt	= time increment;
Δu	= displacement increment
ΔU_{st}	= temperature change for strands;
α_{st}	= thermal expansion coefficient for strands;
$\sigma_t(w)$	= post cracking tensile stress in concrete as a function of opening displacement;
λ	= load proportionality factor.

